Journal of Magnetic Resonance **140,** 442–450 (1999)
Article ID jmre.1999.1864, available online at http://www.idealibrary.com on IDEAL®

High-Resolution Magnetic Resonance Angiography of the Mouse Brain: Application to Murine Focal Cerebral Ischemia Models

Nicolau Beckmann,* Roger Stirnimann,† and Damien Bochelen†

**Core Technologies Area and †Nervous System Department, Novartis Pharma Inc., CH-4002 Basel, Switzerland*

E-mail: nicolau.beckmann@pharma.novartis.com

Received February 19, 1999; revised July 6, 1999

Three-dimensional time-of-flight high-resolution magnetic resonance angiography was applied to visualize the cerebral vasculature of the mouse brain. In normal mice, angiograms of good quality, showing the essential details of the arterial cerebrovascular anatomy, could be obtained in only 2.5 min without the use of contrast agents. Signals from slowly flowing blood, e.g., in veins, could also be detected after administration of a blood pool contrast agent. The technique was applied to mouse models of permanent and transient brain ischemia, involving the occlusion of the middle cerebral artery. High-resolution magnetic resonance angiography proved to be a very useful tool for verifying the success of the occlusion in these models.

Key Words: **angiography; brain; ischemia; magnetic resonance angiography; microscopy; mouse; stroke.**

INTRODUCTION

Magnetic resonance angiography (MRA) has become an established technique in clinical radiology (for a review, see (*1*)). In principle, MRA does not require the application of exogenous contrast agents, since the phase or intensity of the magnetic resonance imaging signal depends on the macroscopic motion of water protons, yielding an intrinsic contrast between the stationary tissue and flowing blood. However, when using contrast agents, MRA may provide also information on blood flow dynamics and on the venous vascular anatomy (*2*).

Despite the increasing importance of MRA in clinics, the method has hardly been used in animal experimentation. The majority of MRA studies involving animals were related to the development of new contrast agents (*3–6*). Some examples of MRA-related vascular imaging in animals are the study of carotid restenosis after balloon angioplasty in rats (*7*), the study of immunological and nonimmunological factors in allo- and autotransplantation of the carotid artery in rats, a new model of chronic graft vessel disease (*8*), the analysis of atherosclerotic lesions in hyperlipidemic rabbits (*9*), and the imaging of the aorta in pigs using intravascular receiver coils (*10*). High-resolution images of vascular wall thickening after removal of the vascular endothelium were obtained in rats using implanted radiofrequency coils (*11*). Further, high-resolution angiograms of the rat cerebral vasculature were recorded using Gd-DTPA as an intravascular contrast agent (*12*). Despite the high quality of the images, this approach is hardly suitable for pharmacological studies due to the long acquisition time of over 7 h. Therefore, recently we have developed techniques for generating high-resolution angiograms of the rat brain without the use of contrast agents (*13*), with acquisition times ranging between 1.25 and 49 min. These techniques were used to obtain angiograms in rat models of focal cerebral ischemia.

Transient middle cerebral artery (MCA) occlusion with the intraluminal thread method for induction of focal ischemia was first used in rats (*14*), and later on refined for application in mice (*15, 16*). The main advantage as compared with other MCA occlusion models is the avoidance of craniotomy and the possibility of reperfusion. Since many factors can lead to inconsistent vascular occlusion, e.g., variable thread diameter and vessel size and biological variability (interindividual and/or strain-related differences), reproducible ischemia requires precise standardization of the experimental conditions. Therefore, it would be highly desirable to be able to verify noninvasively the success of MCA occlusion. In this work we describe the application of high-resolution 3D time-of-flight (TOF) MRA to visualize the cerebral vasculature of the mouse brain, with acquisition times ranging between 2.5 and 24 min. High-resolution angiograms were obtained from normal mice, as well as in mouse models of permanent and temporal occlusion of the MCA by a thread.

MATERIALS AND METHODS

Animals

Male C57 black/6J mice weighing between 22 and 28 g were used throughout the study.

MRA

For the MR investigations, animals were anesthetized with 1.3% forene (Abbott, Cham, Switzerland) in a mixture of

1090-7807/99 $30.00

oxygen/N_2O (1:2) administered via a face mask. The body temperature of the mice was kept at 37°C. No stereotactic holding was used. Measurements were carried out with a Biospec 47/40 spectrometer (Bruker, Karlsruhe, Germany) operating at 4.7 T, equipped with an actively shielded gradient system. The operational software of the scanner was Paravision (Bruker, Karlsruhe, Germany). A 3D gradient-echo sequence with the following imaging parameters was employed: repetition time (TR) = from 12 to 125 ms; echo time (TE) = 1.6 ms; matrix = 96 × 192 × 64; field-of-view (FOV) = 1.44 × 1.92 × 0.64 cm^3. The radiofrequency (RF) pulse was frequency-selective, thereby exciting a coronal slice 0.64 cm thick. Magnetization transfer contrast (MTC) was attained by a frequency-selective Gaussian pulse of 3500 μs duration, with $B_1 = 2$ μT and a frequency offset of 2500 Hz with respect to the water resonance, preceding the 3D gradient-echo sequence by 2.4 ms. An Alderman–Grant-type resonator of 2 cm diameter was used for excitation and detection. The pixel size of the raw data was of 150 × 100 × 100 μm^3; however, all data were zero-filled to $(256)^3$. Angiograms were obtained by generating maximum intensity projections (MIPs) using standard software from the MR system, after zero-filling the raw data.

For contrast agent administration, the tail vein of the mouse was cannulated. A bolus comprising 100 μL of a suspension containing nanoparticles of superparamagnetic iron oxyde (Endorem, Guerbet, Aulnay-sous-Bois, France) at a concentration of 2 mg Fe/mL was injected during 3 s.

Spin-Echo MRI

Spin-echo MRI was carried out 24 h after MCA occlusion, using the following parameters: TR = 2 s; TE = 50 ms; matrix = 256 × 192; FOV = 2.2 × 2.2 cm^2; slice thickness = 0.8 mm; 16 slices.

MCA Occlusion

During surgery, spontaneously breathing mice were anesthetized with 1.5–2% forene (Abbott, Cham, Switzerland) in a mixture of oxygen/N_2O (1:2) administered via a face mask. Body temperature was maintained at 37°C.

Permanent. A vertical 0.5- to 1-cm skin incision was made between the left eye and the ear. The temporalis muscle was exposed and an incision made around its superior margin in order to scrape it from the lateral aspect of the skull. The muscle was then divided by a vertical incision and reflected backward and forward. The exposed MCA was electrocauterized with a small bipolator. The soft tissues were put back into place and the skin was sutured. Immediately after the surgical intervention, mice were placed into the magnet for the acquisition of angiograms.

Transient. After midline neck incision, the right common and external carotid arteries were isolated and ligated. A 6-0 polyester monofilament (diameter of the order of 0.085 mm) coated with silicon resin (RTV coating 3140, Dow Corning, Wiesbaden, Germany) was introduced through a small incision into the internal carotid artery and advanced to a position approximately 9 mm distal from the external carotid artery bifurcation. The silicon resin coated the distal 3 mm of the sutures to a diameter of approximately 0.15 mm. Immediately after the surgical intervention, mice were placed into the magnet for the acquisition of a first series of angiograms. The ischemic period was an hour. Recirculation was achieved by pulling the thread back until its tip had reached the common carotid artery (CCA). By this procedure, blood flow to the ipsilateral MCA was restored from the contralateral carotid artery via the circle of Willis. The incision wound was sutured and the animals were brought back to the magnet for a second examination.

RESULTS

Figure 1 shows maximum intensity projections along the coronal, sagittal and axial directions of an angiogram of the brain of a normal mouse acquired in 16.4 min. The excitation pulse was approximately 45°. The high-resolution angiogram reveals mainly the arterial cerebrovascular anatomy. Venous structures are almost completely suppressed because of the low flow velocity.

Figure 2 shows the effect of the repetition time TR on angiograms acquired from a normal mouse. Also here the excitation pulse was approximately 45°. The main arteries, including the middle cerebral arteries, could be clearly defined already at a TR of 12 ms (acquisition time of 2.5 min). By increasing the TR, flow in more distal parts as well as in extracranial vessels can also be detected.

The effect of the magnetization transfer contrast is illustrated in Fig. 3. An angiogram resulting from a data set acquired at a low flip angle of approximately 20° is presented in Fig. 3a (left). The arterial architecture is barely seen on this angiogram, because the signal from stationary tissue was not sufficiently suppressed. Additional suppression of signals from stationary tissues was achieved by MTC. The angiogram displayed in Fig. 3a (right) was obtained from data acquired at a flip angle of approximately 20°, but with an additional frequency-selective prepulse, irradiated 2500 Hz off resonance. The resulting MTC improved significantly the quality of the angiogram corresponding to the data acquired at a lower flip angle, due to saturation of protons in restricted motion sites. Note that even the branching of the MCA could be detected. By increasing the flip angle of the excitation pulse to approximately 45°, the angiograms without (Fig. 3b, left) and with MTC (Fig. 3b, right) were of equivalent quality. Because of the increased flip angle, the branching of the MCA was not seen on these angiograms.

The angiograms corresponding to Fig. 4 were acquired at a flip angle of approximately 20°, before (Fig. 4a) and 20 min after (Fig. 4b) the injection of contrast agent. The branching of the MCA can be seen on both angiograms; however, following

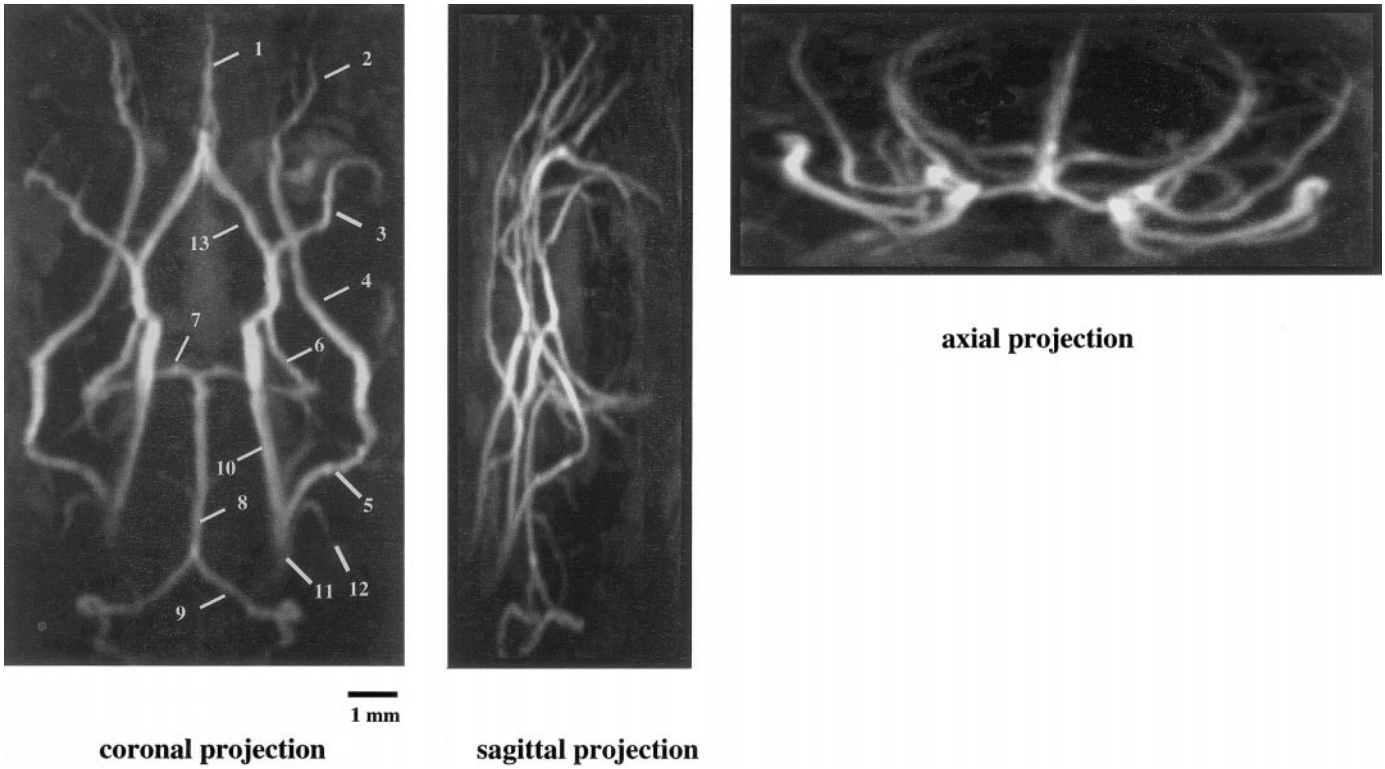

FIG. 1. Coronal, sagittal and axial MIPs of a 3D TOF angiogram of a normal mouse brain, acquired in 16.4 min (TR = 40 ms, TE = 1.6 ms, two averages, excitation pulse of approximately 45°). (1) Anterior cerebral artery; (2) ophthalmic artery; (3) middle cerebral artery; (4) palatine portion of pterygopalatine; (5) pterygo portion of pterygopalatine; (6) posterior cerebral artery; (7) superior cerebellar artery; (8) basilar artery; (9) vertebral artery; (10) internal carotid artery; (11) common carotid artery; (12) external carotid artery; and (13) circle of Willis.

the administration of contrast agent, also venous structures became visible.

The results displayed in the next figures correspond to purely TOF MRA data acquired at a flip angle of approximately 45°. Figure 5 shows a high-resolution angiogram of the cerebrovascular system of the mouse brain, acquired 15 min after permanent occlusion of the MCA. Note the absence of flow in the occluded MCA and also in the posterior cerebral artery. The infarct was confirmed by T_2-weighted spin-echo images, acquired 24 h postoperative (data not shown).

An angiogram of the cerebrovascular system of the mouse brain acquired 15 min after occlusion of the MCA by a thread is shown in Fig. 6a. Note the absence of flow on the occluded MCA and in the internal carotid artery; i.e., flow on the ipsilateral part of the circle of Willis was interrupted by the thread. Due to the surgical procedure, the ipsilateral extracranial vessels remained permanently occluded. After pulling the thread following an ischemic period of 1 h, flow on the MCA was restablished (Fig. 6b). However, signal intensity was lower than on the contralateral MCA, indicating a slight reduction on blood flow after reperfusion. The infarcted region was verified by T_2-weighted spin-echo imaging 24 h after occlusion (Fig. 6c). Infarcts encompassed typically the territory supplied by the MCA, i.e., striatum and frontoparietal cortex.

Figure 7 shows an angiogram acquired 15 min after introduction of a thread. In this case, the surgical intervention was not successful, since the ipsilateral MCA was not occluded. In this animal, no infarct was detected 24 h after the surgical intervention (data not shown). In all mice that presented a remaining flow in the MCA because of misplacement of the thread, no infarcted region was detected 24 h later.

DISCUSSION AND CONCLUSIONS

High-resolution 3D angiograms of the mouse cerebrovascular system were obtained in measurement times between 2.5 and 25 min, without the use of contrast agent. In normal mice, angiograms generated within 2.5 min (TR of 12 ms) showed the principal arteries, including the MCAs. By increasing TR, flow in more distal parts could also be detected. Despite the fact that suppression of stationary signals should be less effective with increasing TR, for an excitation pulse of approximately 45° signal from stationary tissue was efficiently suppressed at all repetition delays used in this study, allowing detection of the vascular (arterial) structures with high contrast. In principle, no additional suppression scheme, e.g., applying magnetization transfer saturation prior to the excitation pulse (*17, 18*) or additional fat suppression (*19*), was required. How-

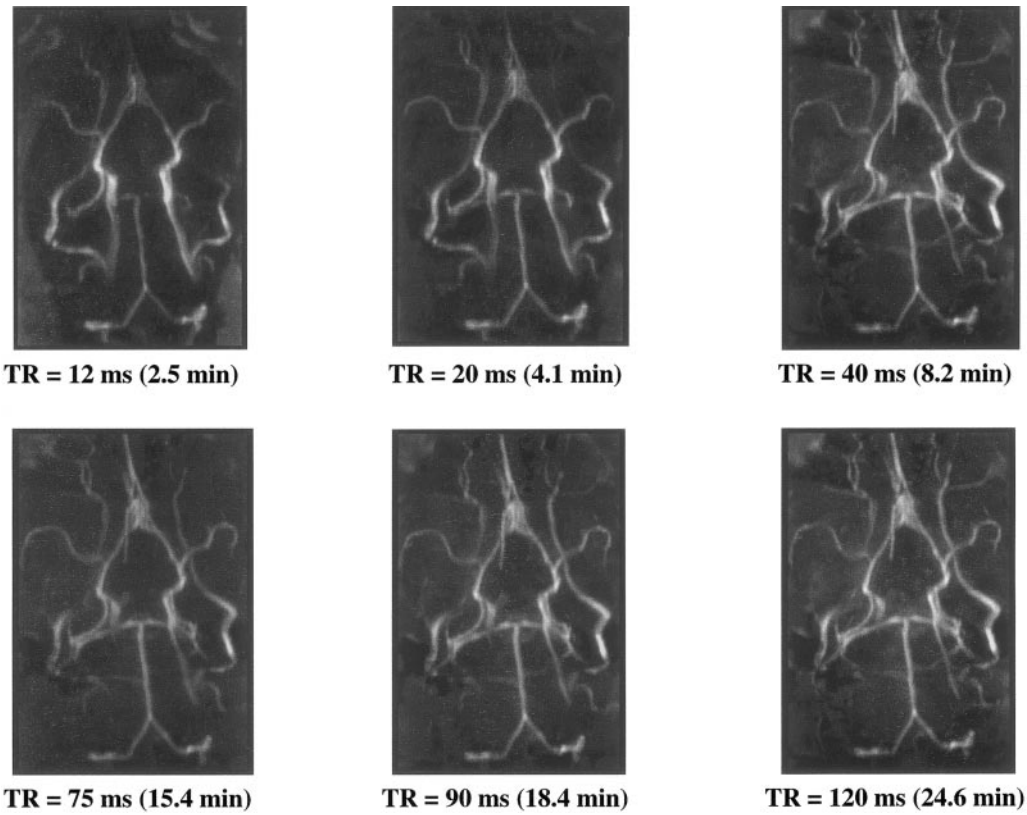

FIG. 2. Coronal MIPs of 3D TOF angiograms of a normal mouse brain, acquired with different repetition times (TR). For each acquisition, TE was 1.6 ms, one average was taken, and the excitation flip angle was of the order of 45°. The total acquisition time for each high-resolution 3D angiogram is indicated in parentheses.

ever, introduction of MTC and administration of a blood pool contrast agent allowed further refinement of the structure of the angiograms (see discussion below).

When using TOF techniques with short TR values, signals from both stationary tissues and slowly flowing venous blood are saturated or suppressed. TOF MRA without the use of contrast agents is sensitive to fast flowing blood, as only unsaturated blood entering the imaging volume between subsequent RF pulses produces high signal. By varying TR, some qualitative information on flow velocities can be obtained, especially in the case of ischemic animals (*4, 13*). The disadvantage is that slowly flowing blood is more difficult to detect by just applying TOF techniques. When blood in the region-of-interest is not completely exchanged during TR, low flip angle RF pulses have to be used in order to provide optimal signal intensity. In this case, the quality of the angiograms can become compromised due to insufficient saturation of signals from stationary tissues. Indeed, when the flip angle of the excitation pulse was reduced to about 20°, the overall quality of the angiograms decreased because of the insufficient suppression of signals from stationary tissues in the TOF experiment (see Fig. 3a). However, introduction of MTC allowed an adequate suppression of stationary signals even at a low flip angle excitation pulse (see Fig. 3b). For larger flip angles, e.g., 45°, angiograms acquired with and without MTC were of similar quality. Therefore, the combination of MTC with a low flip angle excitation pulse was optimal, allowing even the detection of the branching of the MCA.

Detection of slowly flowing blood was further improved by the administration of superparamagnetic iron oxide nanoparticles, a blood pool contrast agent originally developed as a T_2 contrast agent for imaging the reticuloendothelial system (*20–22*). This class of agents has also been found to decrease T_1, and has therefore been used for MR angiography (*23–25*). By remaining in the vascular bed and reducing T_1, also slowly flowing blood, e.g., in veins could be detected (see Fig. 4). However, the concentration of the contrast agent had to be carefully chosen, in order that no predominant reduction in T_2* was obtained.

Although focal cerebral ischemia models in rats have been well documented, descriptions of murine models of MCA occlusion and the experimental difficulties associated with them are scant. Recently, Connolly *et al.* (*26*) provided a detailed description of the surgical technique for either permanent or transient intraluminal MCA occlusion, revealing important differences among strains commonly used in the production of transgenic mice. Kitagawa *et al.* (*27*) showed that strain-related differences in the vascular archi-

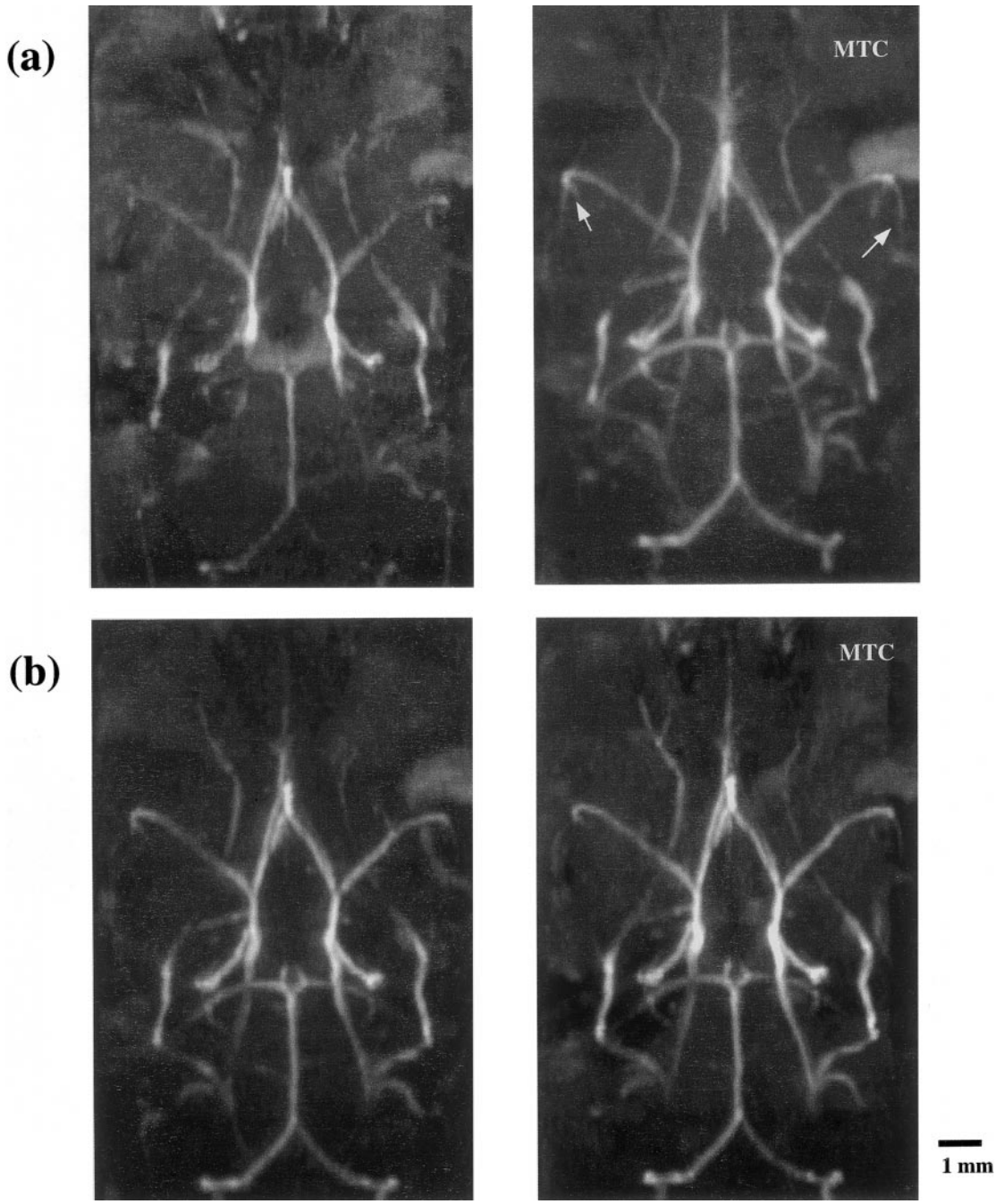

FIG. 3. Coronal MIPs of 3D angiograms of a normal mouse brain, acquired without (left-hand side) and with (right-hand side) MTC. For each acquisition, TE was 1.6 ms, TR was 40 ms, and one average was taken, resulting in a total acquisition time of 8.2 min. MTC was achieved by introducing a frequency-selective prepulse, irradiated 2500 Hz off resonance. The flip angles of the excitation pulse were approximately 20° (a) and 45° (b).

tecture result in important variability in the outcome of MCA occlusion with the intraluminal thread (see next paragraph). In addition to strain-related differences, infarct volume, neurological outcome, and cerebral blood flow appear to be importantly affected by temperature during the ischemic and postischemic periods, mouse size, and size of the suture that obstructs the vascular lumen. Hata *et al.* (*28*) showed that, by matching the diameter of the thread to the weight of the mouse, the reproducibility of cerebral infarction could be improved. These reports point to the difficulties in achieving a consistent vascular occlusion in mice, and that reproducible ischemia requires precise standardization of the experimental conditions. The data presented here show that high-resolution MRA can be applied to verify the

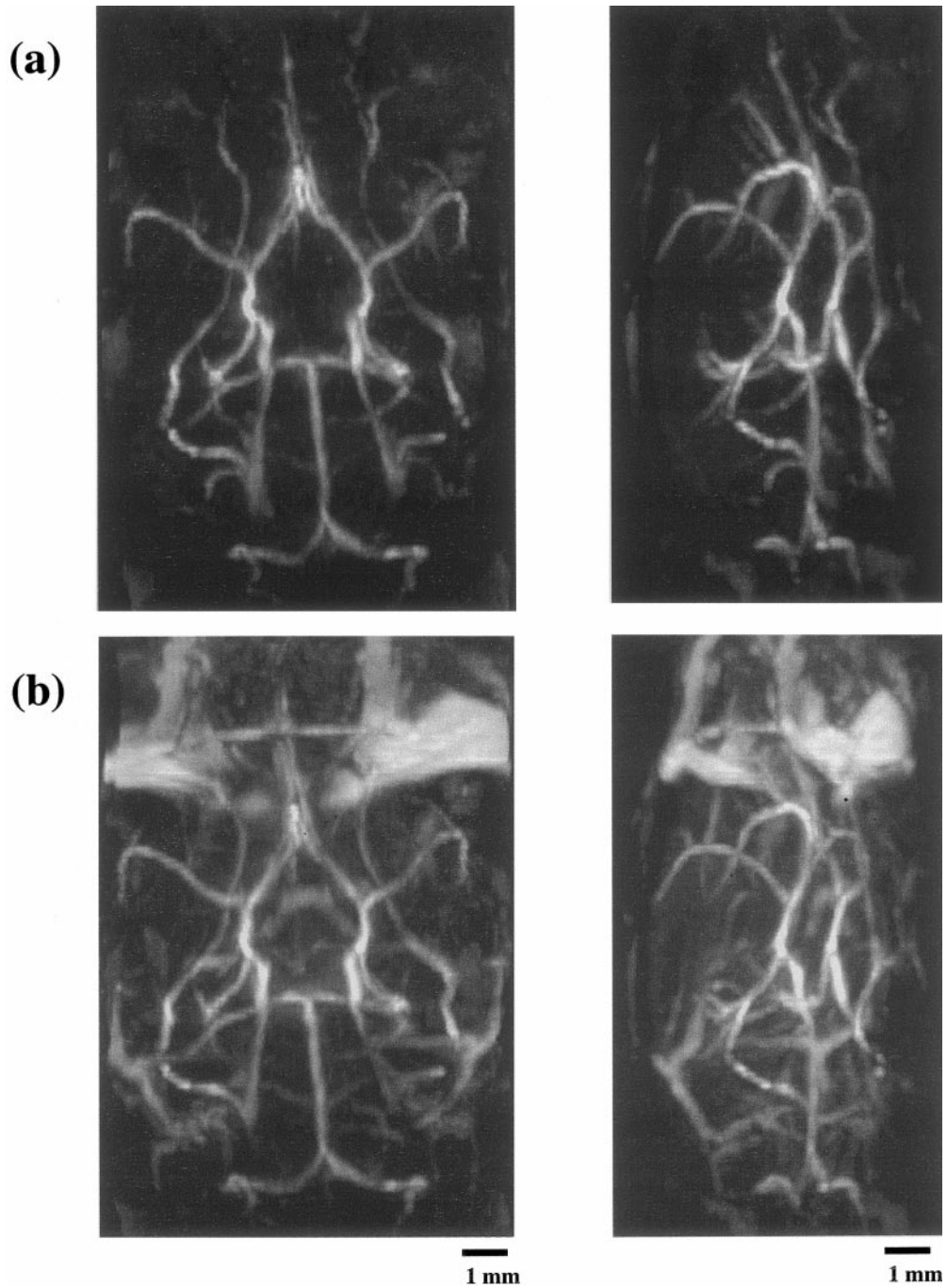

FIG. 4. MIPs of 3D angiograms of a normal mouse brain, acquired previous to (a) and 20 min after (b) contrast agent administration. For each acquisition, TE was 1.6 ms, TR was 40 ms, two averages were taken (resulting in a total acquisition time of 16.4 min), and the excitation flip angle was approximately 20°. MTC was achieved by introducing a frequency-selective prepulse, irradiated 2500 Hz off resonance. The projections on the right-hand side are shifted by 72° with respect to the coronal projections on the left-hand side.

success of MCA occlusion; therefore, it can contribute to standardizing the experimental procedures for murine brain ischemia models.

Transgenic mice are playing an increasing role in stroke research since the discovery that numerous genes are induced by cerebral ischemia, such as genes encoding the heat shock protein hsp72 (*29*), the cytokines interleukin 1, interleukin 6, and tumor necrosis factor α (*30, 31*), and the immediate-early genes *c-fos*, *c-jun*, and *junB* (*32*). The availability of knockout/transgenic technology in the mouse, allowing easy manipulations of gene expressions and their particular translational products in this species, has opened the door to the study of the effects of specific

FIG. 5. Coronal MIP of a 3D TOF angiogram of the mouse brain, acquired 15 min after permanent occlusion of the left MCA (TR = 40 ms, TE = 1.6 ms, one average, excitation pulse of approximately 45°, 8.2 min acquisition time).

gene products on the pathophysiology of stroke. Transgenic mice are being used to investigate ischemia-induced genomic responses in the brain, in order to clarify the mechanisms of inherent degenerative or protective processes and to define targets for specific modulations of these cellular responses. The effect of cerebral ischemia in such mutants has been described in a number of reports, e.g., to assess the effect of the protein p53, a major determinant of the cellular mechanisms that lead to programmed cell death, after an ischemic event (*33*), and to study the role that superoxide radicals (*34*, *35*), tumor necrosis factor α (*36*) and neutrophil adhesion play in the pathogenesis of cerebral infarction (*37*). As transgenic mice are costly and relatively difficult to generate, the use of high-resolution MRA to verify the success of MCA occlusion in ischemic models involving these animals is even more advantageous, because repeated measurements are possible, and in principle there is no requirement for contrast agent administration.

However, Kitagawa *et al.* (*27*) called attention to the fact that differences in vascular anatomy have to be taken into account when cerebral ischemia is produced in a transgenic or knockout mouse. In particular, they showed that the patency of the posterior communicating artery, which connects the superior cerebellar and the posterior cerebral arteries, is crucial in determining the ischemic area after intraluminal suture occlusion. The degree of anastomosis between carotid and vertebrobasilar circulation at the circle of Willis can affect the outcome of an intraluminal occlusion. This anastomosis, although being always present in rats, is highly variable and strain-dependent

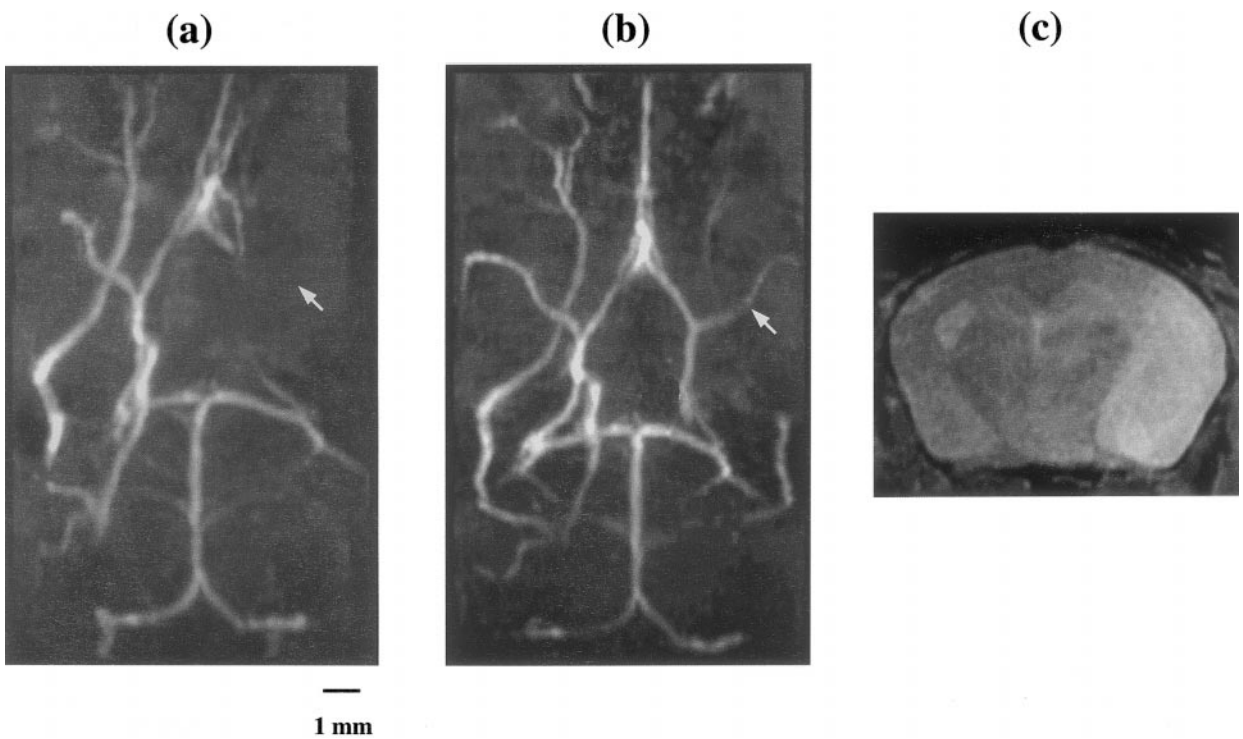

FIG. 6. (a) Coronal MIPs of 3D TOF angiograms of the mouse brain, acquired (a) 15 min after transient occlusion of the right MCA and (b) at reperfusion, 60 min postocclusion (TR = 40 ms, TE = 1.6 ms, one average, excitation pulse of approximately 45°, 8.2 min acquisition time). (c) Spin-echo image acquired 24 h postocclusion, to confirm the infarcted region (TR = 2 s, TE = 50 ms).

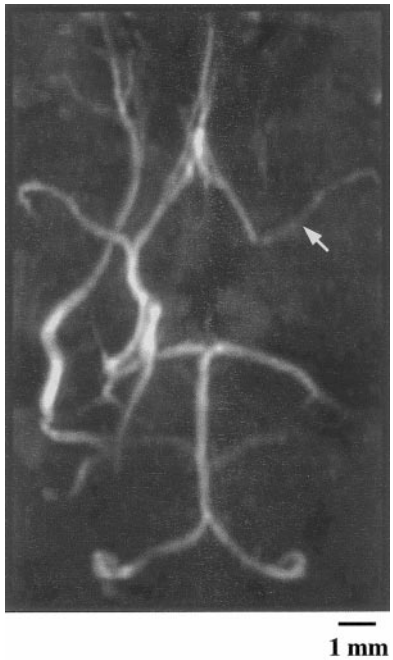

FIG. 7. Coronal MIP of a 3D TOF angiogram of the mouse brain, acquired 15 min after introduction of a thread into the internal carotid artery (TR = 40 ms, TE = 1.6 ms, one average, excitation pulse of approximately 45°, 8.2 min acquisition time). Note that the thread was not advanced enough to occlude the MCA.

in mice (*38*). In the case of intraluminal occlusion, when the thread enters into the anterior cerebral artery and shuts off the blood flow from the ipsilateral carotid circulation, the ipsilateral posterior cerebral artery could be supplied mainly by the basilar artery through the posterior communicating artery. If the communicating artery is absent or poorly developed, the territory supplied by the posterior cerebral artery (i.e., hippocampus and thalamus) would experience ischemia by insertion of the thread into the anterior cerebral artery. Kitagawa *et al.* (*27*) have shown using India ink perfusion that the posterior communicating artery is poorly developed in the C57BL/6 strain, i.e., it is present only on one side of the circle of Willis and with a diameter of less than one third of that of the basilar artery. At the spatial resolution achieved in this study, the posterior communicating artery was not seen on the angiograms even at longer TR and after injection of contrast agent. The posterior communicating artery could be possibly detected by sacrificing temporal resolution in favor of spatial resolution. Here, we tried to keep the acquisition time for an angiogram as short as possible, since we were mainly interested in verifying the success of the surgical intervention and of reperfusion at the level of the MCA only. However, the specific question of the posterior communicating deserves careful further studies, especially when comparing the vascular architecture of different mouse strains. Indeed, determining whether the posterior communicating arteries are present could be of help in selecting the animals and/or the side for performing the surgery, if also the territory supplied by the posterior cerebral artery is aimed at becoming ischemic. Upon such identification, one would perform the occlusion on the side with the poorly developed posterior communicating artery. Presurgery MRA evaluation would limit the need of *postmortem* analysis of the tissue. Such preservation of the tissue could be important if other histological analysis is called for.

In conclusion, we have demonstrated that with 3D TOF MRA high-resolution angiograms of the mouse brain can be obtained without the use of contrast agents, yielding essentially arterial structures. Depending on TR, acquisition times range between 2.5 and 24 min. The main arteries of the mouse brain vasculature, including the MCA, can be clearly defined within a measurement time of 2.5 min. High-resolution MRA proved to be a very useful tool for verifying the success of surgical intervention in murine models of brain ischemia.

ACKNOWLEDGMENTS

The authors acknowledge Dr. Markus Rudin and Dr. Andrè Sauter, from Novartis Pharma, for useful comments about the manuscript, and Konrad Bruttel for technical support.

REFERENCES

1. R. R. Edelman, MR angiography: Present and future, *Am. J. Roentgenol.* **161,** 1–11 (1993).
2. S. L. Talagala, C. A. Jungreis, E. Kanal, S. P. Meyers, T. K. Foo, R. A. Rubin, and G. R. Applegate, Fast three-dimensional time-of-flight MR angiography of the intra-cranial vasculature, *J. Magn. Reson. Imaging* **5,** 317–323 (1995).
3. S. C. Wang, M. G. Wikstrom, D. L. White, *et al.,* Evaluation of Gd-DTPA labeled dextran as an intravascular contrast agent: Imaging characteristics in normal rat tissues, *Radiology* **175,** 280–283 (1990).
4. G. Marchal, H. Bosmans, P. van Hecke, Y. B. Jiang, P. Aerts, and H. Bauer, Experimental Gd-DTPA polylysine enhanced MR angiography: Sequence optimization, *J. Comput. Assist. Tomogr.* **15,** 711–715 (1991).
5. A. A. Bogdanov Jr., R. Weissleder, H. W. Frank, A. V. Bogdanov, N. Nossif, B. K. Schaffer, E. Tsai, M. I. Papisov, and T. J. Brady, A new macromolecule as a contrast agent for MR angiography: Preparation, properties and animal studies, *Radiology* **187,** 701–706 (1993).
6. J. C. Bock, U. Pison, F. Kaufmann, and R. Felix, Gd-DTPA-polylysine-enhanced pulmonary time-of-flight MR angiography, *J. Magn. Reson. Imaging* **4,** 473–476 (1994).
7. N. S. Cook, H.-G. Zerwes, C. Pally, M. Rudin, and R. P. Hof, Spirapril and cilazapril inhibit neointimal lesion development but cause no detectable inhibition of lumen narrowing after carotid artery balloon catheter injury in the rat, *Blood Pressure* **2,** 322–331 (1993).
8. S. Wehr, M. Rudin, J. Joergensen, A. Hof, and R. P. Hof, Allo- and autotransplantation of carotid artery–A new model of chronic graft vessel disease, *Transplantation* **64,** 20–27 (1997).
9. C. Yuan, M. P. Skinner, E. Kaneko, L. M. Mitsumori, C. E. Hayews, E. W. Raines, J. A. Nelson, and R. Ross, Magnetic resonance imaging to study lesions of atherosclerosis in the hyperlipidemic rabbit aorta, *Magn. Reson. Imaging* **14,** 93–102 (1996).

10. A. J. Martin and R. M. Henkelman, Intravascular MR imaging in a porcine animal model, *Magn. Reson. Med.* **32,** 224–229 (1994).
11. L. Arnder, X. Zhou, G. P. Cofer, L. W. Hedlund, and G. A. Johnson, Magnetic resonance microscopy of the rat carotid artery at 300 MHz, *Invest. Radiol.* **29,** 822–826 (1994).
12. A. F. Mellin, G. P. Cofer, B. R. Smith, S. A. Suddarth, L. W. Hedlund, and G. A. Johnson, Three dimensional magnetic resonance microangiography of rat neurovasculature, *Magn. Reson. Med.* **32,** 199–205 (1994).
13. T. Reese, D. Bochelen, A. Sauter, N. Beckmann, and M. Rudin, Magnetic resonance angiography of the rat cerebrovascular system without the use of contrast agents, *NMR Biomed.* **12,** 189–196 (1999).
14. J. Koizumi, Y. Yoshida, T. Nakazawa, and G. Oneda, Experimental studies of ischemic brain edema. 1. A new experimental model of cerebral embolism in rats in which recirculation can be introduced in the ischemic area, *Jpn. J. Stroke* **8,** 1–8 (1986).
15. H. Kamii, H. Kinouchi, F. R. Sharp, C. J. Epstein, S. M. Sagar, and P. H. Chan, Expression of c-fos mRNA after a mild focal cerebral ischemia in SOD-1 transgenic mice, *Brain Res.* **662,** 240–244 (1994).
16. H. Hara, P. L. Huang, N. Panahian, M. C. Fishman, and M. A. Moskowitz, Reduced brain edema and infarction volume in mice lacking the neuronal isoform of nitric oxide synthase after transient MCA occlusion, *J. Cereb. Flow Metab.* **16,** 605–611 (1996).
17. B. Pike, B. S. Hu, G. H. Glover, and D. R. Enzmann, Magnetization transfer time-of-flight magnetic resonance angiography, *Magn. Reson. Med.* **25,** 372–379 (1992).
18. R. R. Edelman, S. S. Ahn, D. Chien, W. Li, A. Goldmann, M. Mantello, J. Kramer, and J. Kleefield, Improved time-of-flight angiography of the brain with magnetization transfer contrast, *Radiology* **184,** 395–399 (1992).
19. W. Lin, J. A. Tkach, E. M. Haacke, and T. J. Marsaryk, Intracranial MR angiography: Application of magnetization transfer contrast and fat saturation to short gradient echo, velocity-compensated sequences, *Radiology* **186,** 753–761 (1993).
20. R. Weissleder, G. Elizondo, J. Wittenberg, C. Rabito, H. Bengele, and L. Josephson, Ultrasmall superparamagnetic iron oxide: Characterization of a new class of contrast agents for MR imaging, *Radiology* **175,** 489–493 (1990).
21. P. J. Mergo, T. Helmberger, A. I. Nicolas, and P. R. Ros, Ring enhancement in ultrasmall superparamagnetic iron oxide MR imaging: A potential new sign for characterization of liver lesions, *Am. J. Roentgenol.* **166,** 379–384 (1996).
22. M. G. Harisinghani, S. Saini, R. Weissleder, *et al.,* Differentiation of liver hemangiomas from metastases and hepatocellular carcinoma at MR imaging enhanced with blood-pool contrast agent Code-7227, *Radiology* **202,** 687–691 (1997).
23. Y. Anzai, M. R. Prince, T. L. Chevenert, *et al.,* MR angiography with an ultrasmall superparamagnetic iron oxide blood pool agent, *J. Magn. Reson. Imaging* **7,** 209–214 (1997).
24. W. Mayo-Smith, S. Saini, G. Slater, J. Kaufman, P. Sharma, and P. Hahn, MR contrast for vascular enhancement: Value of superparamagnetic iron oxide, *Am. J. Roentgenol.* **166,** 73–77 (1996).
25. A. Stillman, N. Wilke, D. Li, M. Haacke, and S. McLachlan, Ultrasmall superparamagnetic iron oxide to enhance MRA of the renal and coronary arteries: Studies in human patients, *J. Comput. Assist. Tomogr.* **20,** 51–55 (1996).
26. E. S. Connolly Jr., C. J. Winfree, D. M. Stern, R. A. Solomon, and D. J. Pinsky, Procedural and strain-related variables significantly affect outcome in a murine model of focal cerebral ischemia, *Neurosurgery* **38,** 523–531 (1996).
27. K. Kitagawa, M. Matsumoto, G. Yang, T. Mabuchi, Y. Yagita, M. Hori, and T. Yanagihara, Cerebral ischemia after bilateral carotid artery occlusion and intraluminal suture occlusion in mice: Evaluation of the patency of the posterior communicating artery, *J. Cereb. Flow Metab.* **18,** 570–579 (1998).
28. R. Hata, G. Mies, C. Wiessner, K. Fritze, D. Hesselbarth, G. Brinker, and K.-A. Hossmann, A reproducible model of middle cerebral artery occlusion in mice: Hemodynamic, biochemical, and magnetic resonance imaging, *J. Cereb. Flow Metab.* **18,** 367–375 (1998).
29. H. Kinouchi, F. R. Sharp, J. Koistinaho, K. Hicks, H. Kamii, and P. H. Chan, Induction of heat shock hsp70 mRNA and HSP70 kDa protein in neurons in the "penumbra" following focal cerebral ischemia in the rat, *Brain Res.* **619,** 334–338 (1993).
30. C. Wiessner, J. Gehrmann, D. Lindholm, R. Topper, G. W. Kreutzberg, and K.-A. Hossmann, Expression of transforming growth factor-beta 1 and interleukin-1 beta mRNA in rat brain following transient forebrain ischemia, *Acta Neuropathol.* **86,** 439–446 (1993).
31. M. Buttini, K. Appel, A. Sauter, H. P. Gebicke, and H. W. Boddeke, Expression of tumor necrosis factor alpha after focal cerebral ischemia in the rat, *Neuroscience* **71,** 1–16 (1996).
32. H. Kinouchi, F. R. Sharp, P. H. Chan, J. Koistinaho, S. M. Sagar, and T. Yoshimoto, Induction of c-fos, junB, c-jun, and hsp70 mRNA in cortex, thalamus, basal ganglia, and hippocampus following middle cerebral artery occlusion, *J. Cereb. Flow Metab.* **14,** 808–817 (1994).
33. R. C. Crumrine, A. L. Thomas, and P. F. Morgan, Attenuation of p53 expression protects against focal ischemic damage in transgenic mice, *J. Cereb. Flow Metab.* **14,** 887–891 (1994).
34. G. Yang, P. H. Chan, J. Chen, E. Carlson, S. F. Chen, P. Weinstein, C. J. Epstein, and H. Kamii, Human copper–zinc superoxide dismutase transgenic mice are highly resistant to reperfusion injury after focal cerebral ischemia, *Stroke* **25,** 165–170 (1994).
35. P. H. Chan, H. Kamii, G. Yang, J. Gafni, C. J. Epstein, E. Carlson, and L. Reola, Brain infarction is not reduced in SOD-1 transgenic mice after a permanent focal cerebral ischemia, *Neuroreport* **5,** 293–296 (1993).
36. A. J. Bruce, W. Boling, M. S. Kindy, J. Peschon, P. J. Kraemer, M. K. Carpenter, F. W. Holtsberg, and M. P. Mattson, Altered neuronal and microglial responses to excitotoxic and ischemic brain injury in mice lacking TNF receptors, *Nature Med.* **2,** 788–794 (1996).
37. E. S. Connolly Jr., C. J. Winfree, T. A. Springer, Y. Naka, H. Liao, S. D. Yan, D. M. Stern, R. A. Solomon, R. J. Gutierrez-Ramos, and D. J. Pinsky, Cerebral protection in homozygous null ICAM-1 mice after middle cerebral artery occlusion. Role of neutrophil adhesion in the pathogenesis of stroke, *J. Clin. Invest.* **97,** 209–216 (1996).
38. F. C. Barone, D. J. Knudsen, A. H. Nelson, G. Z. Feuerstein, and R. N. Villette, Mouse strain differences in susceptibility to cerebral ischemia are related to cerebral vascular anatomy, *J. Cereb. Flow Metab.* **13,** 683–692 (1993).